

1 **Measurement and self-operating computer of the leukocyte continuum as a fixed space–**
2 **time continuum in inflammation**

3 **Running title:** Biomarker by smoothness equation and coordinate system

4 Yuusuke Nonomura

5 Nonomura Dental Clinic, National Yagata Bldg 2F, Nagoya City, Japan

6

7 **To whom correspondence should be addressed:**

8 Yuusuke Nonomura

9 Nonomura Dental Clinic, National Yagata Bldg 2F 3-6, Higasiyamatoori, Chikusa-ku, Nagoya

10 City, Aichi 4640807, Japan

11 Tel: +81-52-781-4185

12 Fax: +81-52-781-4185

13 E-mail: n-dent@tulip.ocn.ne.jp

14

15 **Abstract**

16 **Motivation:** No biomarkers and systems, including leukocyte count and flow cytometry, can be
17 used to measure tissue injury for diagnosing inflammation. A fixed space–time continuum ($S\tau C$)
18 biomarker can address this issue. A leukocyte continuum (LC) is a biomarker forming a $S\tau C$
19 capable of measuring injury by operators and equations for a self-operating computation.

20 **Results:** A self-operating computer (SOC) LC as a water treatment for leukocyte(s) was generated
21 using leukocyte(s). String leukocyte continuum (StrLC), single-layer leukocyte (SLL) and
22 multilayer leukocyte continuum (MLC) were demonstrated in various LCs using an equation
23 with a primitive-operator. In the SOC, the LC is the inflammation graph of the operation result.
24 The relative differential equation (RDE) shows how to recognize the LC not as a ‘model’ in the
25 conventional-other-operating-computer (cOOC), but as an actual arithmetic unit with a display
26 unit. The SOC shows the essential nature in real time.

27

28 INTRODUCTION

29 An other-operating computer (OOC) is a computer comprising NAND and NOR silicon logic
30 chip that performs processing using algorithms on these circuits and displays graphs upon
31 analogue-to-digital (A/D) conversion of sample information. Conventional natural phenomena
32 are mainly analysed via cOOC, which considers the solution of the conventional
33 convergence-differential equation (CDE) as the core (Example S1). However, the cOOC cannot
34 calculate an absolute origin (AO) (singularity) at the boundary of multiple quadrants {an
35 example is the problem of inconsistency in the directional properties associated with the
36 equation-of-motion (IDP-EOM)}, different-object interference (AO) (singularity) (an example is
37 the prey and predator problem) (Britton, 2010; Hawkins, 1999; Krainov, 2002; Teramoto, 2009;
38 Thornley, 2007) and relative origin (RO) (singularity) (Saw, E.-W., et al., 2016). AO and RO do
39 not have smoothness (Text S1). Their singularities are the origin of the problems that follow (e.g.
40 non-calculable inflammation). Therefore, the conventional scientific method (e.g. Text S2-4,
41 Material S1) only has the OOC until the end of this paper.

42 However, a self-operating computer (SOC) is the phenomenon itself that is recognized
43 to be arithmetic circuit {by relative-differential equation: RDE (Definition S6)} with graphic
44 display function { $D()$ or $D(N())$ } unlike the OOC. In SOC RDE and OOC by SOC, AO and RO
45 (Definition S6.4) are calculable and smooth. { $D()$ is an image device function (microscope, MRI,

46 CT, telescope, etc.); $N()$ is the function indicating diffusion extent from tissue injury and that of
47 the samples (on glass slide) covered with a glass cover.

48 One example is the Navier–Stokes equation (NSE) generated using the RDE. The
49 observation image is $D(\text{RDE})$ or $D(N(\text{RDE}))$. When sampling a tissue injury and making a direct
50 observation, one directly observes the RDE arithmetic result. The SOC consists of the formation
51 of a fixed space–time continuum ($S\tau C$) by an observed object and from the RDE that shows the
52 SOC. The solution takes $k\text{OOC}$ and $z\text{OOC}$. The SOC shows inflammation, elementary particle,
53 life, and new figure of the space–time continuum. Inflammation is one such example of the SOC.
54 The directional property that measures decomposed single cell, including cell injury, takes the
55 direction of modern pathology, and is indicated in a (blood) cell-counting system (Graham et al.,
56 2003), a cell measurement system as flow cytometry (FCM) (Cossarizza et al., 2017) and
57 leukocyte counts (Lcnt) (Saito, 2002; DACIE, 1975). This is defined as “cell (injury) element
58 theory” (CET). The method describes the royal road of the OOC consisting of decomposition
59 into element (cell) from a sample and analysis (operation processing) of the sample. Per cell
60 decomposition destroys the tissue structure (tissue injury). Cell injury cannot measure
61 inflammation, which is the best biomarker of an invasive disease. However, it can be measured
62 with tissue injury and understood by observations of tissue sections (Rubin, 2007). Therefore, in
63 the conventional system, the space–time continuum information of tissue injury is destroyed

64 because it decomposes into a cell and measured. The structure is also destroyed if leukocytes
65 from multi-tissue injury are mixed by the observer. Both cause the destruction of the structure,
66 especially statistical sampling. In modern pathology, the CET faces problems. However, the
67 leukocyte continuum (LC) as $S\tau C$ as RDE, which realises the SOC, solves the problems of
68 structural bioinformatics and enables the measurement of local inflammation and tissue
69 information. The problems encountered are 1) lack of structure of bio-information, which can
70 measure the space of inflammation over time {problem of cell/tissue injury (cell/tissue
71 information) }; 2) destruction of the structure of bio-information by statistical sampling; 3) lack
72 of smoothness of differentiation; 4) problem of the simultaneous differential equation (SDE) (prey
73 and predator, etc.); and 5) the problem that cannot be visually quantified by a doctor.

74 **SYSTEM AND METHODS**

75 **Materials**

76 In my clinic, the LC was based on the finding that was incidentally discovered in the
77 microscopic examination of periodontitis (infection). Microbial culture and microscopic
78 examination to the infection were also performed in the clinic. {I have posted using the finding
79 for journal, and such as society, on the noticeboard of my clinic for progress of medical science
80 (Text S5).}

81 The LC had the SOC as the material. The SOC was built as a continuum formation by water

82 treatment of leukocyte(s) as an arithmetic circuit material. The RDE was the method used to read
83 the LC. Meanwhile, kOOC (OOC with Kyoku), zOOC (OOC with Zai) and kzOOC (OOC with
84 Kyoku and Zai) were the solutions used for the SOC. The RDE (Definition S6) is composed of
85 Zai and Kyoku, which was a primitive-operator (Definitions S1–6). In the microscopic
86 examination, a multicircle explorer (MCE; Isizuka Co., Ltd., Japan; Figure S1) was used to
87 sample the gingival crevicular fluid (GCF) using glass slides, cover glasses, a phase-contrast
88 microscope and a fluorescence microscope (Limited company, MicroDent, Japan). The OOC
89 used a general-purpose PC, picture processing software and arithmetic software.

90 **Methods**

91 *Conservative sampling, water operation and generation of the WSTLs/WTLs*

92 The GCF from the periodontal pocket of patients with periodontitis was conservatively sampled
93 using an MCE (Figure S1) and transferred to glass slides. Accordingly, 20 μ L of water (water
94 treatment of leukocyte: WTL) and 20 μ L of acid red aqueous solution (0.1 wt.%) were added
95 (water solution treatment leukocyte: WSTL). The samples were covered with glass cover slips
96 and observed using microscope images {D()} (size: 720 \times 480).

97 Through the water treatment, the mutual leukocytes combined together for a short distance
98 (Figures 1 and S4–S6) and formed the LC, which had $S\tau C$ and τSC . Therefore, the water
99 treatment can prevent the destruction of the space–time structure of the leukocytes from the

100 tissue injury and the destruction by mixing of the leukocytes from the multi tissue-injury. The
101 size was assumed to be proportional to that of the tissue injury because larger leukocytes exist in
102 larger injuries. The larger cluster that exceeds that of a small tissue injury does not exist (Figures
103 1–5 and S2–7).

104 *Time and phase condition of the WSTLs/WTLs*

105 The active leukocytes (ALs; Figure 2), destructive leukocytes (DLs; Figure 3) and LC are
106 presented in Definition S7 (Figures 2–5).

107 *SOC and OOC observation*

108 Reading the SOC image is possible with the RDE (science eye) in the brain (i.e. the SOC
109 recognises the graph as a result of arithmetic, operation and calculation) (Definitions S1–7,
110 Method S1). The OOC was calculated using a common digital computer.

111 **Algorithm**

112 *First algorithm of the arithmetic circuit creation*

113 *Circuit elements*

114 A conventional computer consists of AND, OR and NOT gates in a logical circuit. This
115 leukocyte circuit (LC) as StC consists of Zai and Kyoku (Definitions S1–S3). The
116 WSTLs/WTLs are Zai, and had an inner-space and inner-time. The inner-space herein is ΔN
117 (zero dimensional space; P_0 is the number described in Definitions S1, S3, and S7). The

118 inner-time is $\Delta\tau$ (P_0 is the fixed-time described in Definitions S1, S3 and S7). $ZaiN$ and $Zait$
119 $(\Delta N/\Delta\tau)$ consist of WSTLs/WTLs (Figures S4–7). ' N ' is the number of cells {leukocyte(s) or
120 microorganism(s)}. t_n is the physical time. τ denotes the phase time by a biological activity time
121 (Figure S8, Definitions S1.6 and S7). The changes in the boundaries (as the membranes of cells
122 or nuclei) are the changes of the phase time (the main value of τ is '1'; $\tau = 1$). The boundary
123 defines the inner-Kyoku (iK; Definitions S1–S3). Zai constitutes a real coordinate system (RCS;
124 Figure 6 C3-RCS). C1 RCS and C2 RCS are the components, which did an inheritance
125 derivation from C3 RCS (Definitions S3.6.1 and S6.1 and Figure 6). n and m are the phase
126 values as positive integers (Definition S1). n is origin (relative or absolute), whilst m is
127 non-origin.

128 *Circuit build*

129 Considering whether leukocytes were immersed in water and near tissue injury, the leukocytes
130 were conservatively sampled by the MCE (Figure S1) and immediately immersed in water or
131 water solution (Figures 1, S2, and S3). The microscope images of these leukocytes were then
132 used to generate single-layer leukocytes (SLLs; Figures 2 and 3), string LC (StrLC; Figure 4) and
133 multilayer LC (MLC; Figure 5). These were equivalent to the arithmetic circuit itself, and could
134 be used as the RDE (Definitions S1–S7 and Figures S4–S7). In other words, the equation and the
135 operator(s) that elementised the nature formed the structure of the arithmetic circuit and the

136 resulting graph. The structure forms the arithmetic circuit and the resulting graph if the natural
137 phenomenon is constructed and built on certain conditions. Accordingly, it defined the SOC.

138 The LC in the SOC is defined as $S\tau C$. The LC in the OOC is defined as τSC (Definition
139 S7.2, Figure S7).

140
$$\frac{\Delta space}{\Delta \tau} \quad (SOC) \text{ is } S\tau C. \quad \text{Space} = f(\tau) \quad (OOC) \text{ is } \tau SC.$$

141 The SOC denotes the microscope images that simultaneously provide information on
142 size and form and represent an RDE. In contrast, the OOC is the solution.

143

144 **Various LCs as the SOC as the arithmetic circuit and OOC**

145 *StrLC*

146 *SOC*

147 The StLC is the string LC, whose width \emptyset is one WSTL/WTL. Therefore, the size of the tissue
148 injury, which it indicates, is \emptyset (Figure 4, Table S3). Therefore, t_n denotes the physical time.

149

150 *SOC1 (from CI-RDE)*

151 The injury size is $(N = 1)$, where N is fixed. Therefore, the equation uses time as a variable:

$$152 \quad \left(\frac{\triangle_{n-m} \triangle_n \cdot 1}{\triangle_{n-m} \triangle_n \cdot t} \right) = \frac{\triangle_{n+S_1m} \triangle_n \cdot 1}{\triangle_{n+S_1m} \triangle_n \cdot t} = \frac{\triangle_{n+S_1m} \triangle_n \cdot N}{\triangle_{n+S_1m} \triangle_n \cdot t} = \frac{\triangle_{n+S_1m} \triangle_n \cdot N}{\triangle_{n+S_1m} \triangle_n \cdot n+S_1m t_n}$$

153 A motion object without iK: DL (AL \rightarrow DL):

$$154 \quad \frac{\triangle_{n+S_1m} \triangle_n \cdot 1}{\triangle_{n+S_1m} \triangle_n \cdot t} \rightarrow \frac{S_1 \cdot 1}{\triangle_{n+S_1m} \triangle_n \cdot t} \quad \left(\begin{array}{l} \text{without iK} \\ \text{with iK} \end{array} \right)$$

155 S_1 is defined in Definition S2.

156 *SOC2*

157 Tissue injury form: $D \left(\triangle_{n-m} \triangle_n \right)$, equal to one WSTL/WTL circle form

158 You will observe StrLC as $\triangle_{n-m} \triangle_n$ in the microscopic image in $D \left(\triangle_{n-m} \triangle_n \right)$.

159 *OOC*

$$160 \quad v_m = \frac{\triangle(y_{n+S_1m} - y_n)}{\triangle(t_{n+S_1m} - t_n)} \cong \text{or} = \frac{\left(\triangle_{n+S_1m} \triangle_n N \right) \cdot \emptyset}{\triangle_{n+S_1m} \triangle_n t} \equiv \frac{\triangle(n+S_1m - n)N \cdot \emptyset}{\triangle(n+S_1m - n) \cdot t}$$

$$161 \quad \begin{array}{ccc} \triangle_{S_1} \cdot m \cdot 1 \cdot \emptyset & \xrightarrow{\text{Bundling}} & \triangle \cdot \frac{m \cdot 1 \cdot \emptyset}{m \cdot t} \equiv \triangle \frac{\emptyset}{t} \\ \triangle_{S_1} \cdot m \cdot t & \xleftarrow{\text{Distributing}} & \end{array}$$

162 In StrLC, $N = 1$, n is origin (AO or RO), and \emptyset is one leukocyte diameter.

163 t_x is Kyoku value (x is positive integer), t and $n+S_1m t_n$ are Zai value (Po)

164
$$\Delta(t_{n+S_1m} - t_n) \cong or = {}_{n+S_1m}\Delta_n t \equiv {}_{n+S_1m}\Delta_n \cdot {}_{n+S_1m}t_n$$

165 **Properties**

166 A StrLC from the same injury can be described by the EOM; however, this StrLC biomarker uses
 167 the RCS to represent future inflammation, making it necessary to solve the problem of IDP-EOM
 168 by addressing smoothness. A cOOC expresses only one side. Therefore, it generates singularity
 169 and integration constants (Figure S9, Table S1). The EOM with Str Zai C3-CS (CS: coordinate
 170 system) (Definition S3.6.1, Figure 6, Text S6) is presented as follows:

171
$$\frac{d^2y}{dt^2} = \Delta a \quad \text{and} \quad \frac{d^2y}{dt^2} = \Delta a$$

172 This is only a ‘model’.

173 The OOC with iK are

174 Single Zai: $y_1 = \frac{1}{2}a(t\Delta)^2 + v_0(t\Delta)^1 + y_0(t\Delta)^0$ (1st quadrant)

175 Single Zai: $y_2 = \frac{1}{2}a(t\Delta)^2 + v_0(t\Delta)^1 + y_0(t\Delta)^0$ (2nd quadrant)

176 Above the single Zai is the ω d switch that is ‘ON’. In this case only, t is a variable. The other is
 177 Po (Supplementary Method S1.1). The others are all ‘OFF’. The variable is phase (n and m).

178 Zai continuum:

179 $y_1 = \frac{1}{2}a(\Delta t_{n+m})^2 + v_0(\Delta t_{n+m})^1 + y_0(\Delta t_{n+m})^0$ (Local in 1st quadrant)

180 $y_1 = \frac{1}{2}a(\Delta t_{n+S_2m})^2 + v_0(\Delta t_{n+S_2m})^1 + y_0(\Delta t_{n+S_2m})^0$ (Relative in 1st quadrant)

181 $y_1 = \frac{1}{2}a(\Delta t_{n+m})^2 + v_0(\Delta t_{n+m})^1 + y_0(\Delta t_{n+m})^0$ (Relative in 1st quadrant)

182
$$y_2 = \frac{1}{2}a(\Delta t_{n+m})^2 + v_0(\Delta t_{n+m})^1 + y_0(\Delta t_{n+m})^0 \text{ (Local in 2nd quadrant)}$$

183
$$y_2 = \frac{1}{2}a(\Delta t_{n+S_1m})^2 + v_0(\Delta t_{n+S_1m})^1 + y_0(\Delta t_{n+S_1m})^0 \text{ (Relative in 2nd quadrant)}$$

184
$$y_2 = \frac{1}{2}a(\Delta t_{n-m})^2 + v_0(\Delta t_{n-m})^1 + y_0(\Delta t_{n-m})^0 \text{ (Relative in 2nd quadrant)}$$

185
$$y = y_2 + y_1 \text{ (} y_1 \text{ (1st quadrant) is } S_2 \text{ side, } y_2 \text{ (2nd quadrant) is } S_1 \text{ side)}$$

186 a is the acceleration as Po; v_0 is the velocity as Po; and y_0 is the distance as Po.

187 S_1 and S_2 are the Str operators (Definitions S2 and S3), and the observer in the local field

188 (LF) is denoted as $n + m$. The operation was performed using the LF and the relative field (RF).

189 The observer in the global field (GF) RF is denoted as $n + S_1m$ in the C3-CS, where the

190 independent variables included Δt . n is the absolute or relative origin. Conventionally, at an

191 origin, the direction of motion of the quadratic term is reversed (Figure S9). However, in an RCS,

192 the quadratic term maintains the same direction, and the linear term of the conventional equation

193 and of this equation maintain the same direction (Figures 6 and S10, Table S1).

194 y_x is the diameter \emptyset of the WSTL/WTLs, whilst τ_x is calculated from the activity of the

195 leukocytes. When $y_1 = \emptyset_1$, the velocity is calculated from the solution of the EOM {RF (real

196 field)}:

197
$$v_{m2} = \frac{\Delta(y_{n-m} - y_n)}{\Delta(t_{n-m} - t_n)} = \frac{{}_{n+S_1m}\Delta_n(y_{n+S_1m} - y_n)}{{}_{n+S_1m}\Delta_n(t_{n+S_1m} - t_n)} \text{ (2nd quadrant),}$$

$$198 \quad v_{m1} = \frac{\Delta(y_{n+m} - y_n)}{\Delta(t_{n+m} - t_n)} = \frac{{}_n\Delta_{n+S_2m}(y_{n+S_2m} - y_n)}{{}_n\Delta_{n+S_2m}(t_{n+S_2m} - t_n)} \quad (1\text{st quadrant})$$

199 The object without iK (time has iK) is presented as follows:

$$200 \quad v_{m2} = \frac{S_1 \cdot (y_{n-m} - y_n)}{\Delta(t_{n-m} - t_n)} = \frac{S_1 \cdot y_{n+S_1m} - S_1 \cdot y_n}{{}_{n+S_1m}\Delta_n(t_{n+S_1m} - t_n)} \quad (2\text{nd quadrant})$$

$$201 \quad v_{m1} = \frac{S_2 \cdot (y_{n+m} - y_n)}{\Delta(t_{n+m} - t_n)} = \frac{S_2 \cdot y_{n+S_2m} - S_2 \cdot y_n}{{}_n\Delta_{n+S_2m}(t_{n+S_2m} - t_n)} \quad (1\text{st quadrant})$$

$$202 \quad t_{n+S_2m} \equiv t \cdot (n + S_2m), \quad t_{n+S_1m} \equiv t \cdot (n + S_1m) = t \cdot (n - m)$$

203 y_1, y_2, \dots, y_n is one WSTL diameter, and t_1, t_2, \dots, t_n is the elapsed time of the WSTL. Acceleration

204 is calculated from the solution of the EOM {RF (real field)}:

$$205 \quad a_{m2} = \frac{\Delta(v_{n+S_1m} - v_n)}{\Delta(t_{n+S_1m} - t_n)}, \quad a_{m1} = \frac{\Delta(v_{n+S_2m} - v_n)}{\Delta(t_{n+S_2m} - t_n)}$$

206 where v_1, v_2, \dots, v_n denote velocity, and t_1, t_2, \dots, t_n denote the elapsed time of the WSTLs.

207

208 SLLs (AL or DL)

209 C1-RDE (Definition S6):

$$210 \quad \frac{\tau_n}{Z} = \frac{{}_n\tau}{Z} = \frac{r dN_{\tau_n}}{r d\tau_n} = \frac{{}_{n-m}\Delta_n N_{2\tau}}{{}_{n-m}\Delta_n \tau} - \frac{{}_n\Delta_{n+m} N_{1\tau}}{{}_n\Delta_{n+m} \tau} = + \frac{{}_{n+S_1m}\Delta_n N_{2\tau}}{{}_{n+S_1m}\Delta_n \tau} + \frac{{}_n\Delta_{n+S_2m} N_{1\tau}}{{}_n\Delta_{n+S_2m} \tau}$$

211 Detail:

$$\begin{aligned}
 & \frac{\binom{n+S_1m}{n} N_2}{\binom{n+S_1m}{n} \cdot n^{n+S_1m} \tau^n} - \frac{\binom{n+S_2m}{n} N_1}{\binom{n+S_2m}{n} \cdot n^{n+S_2m} \tau^n} \\
 & = \frac{\binom{n+S_1m}{n} N_2}{\binom{n+S_1m}{n} \cdot n^{n+S_1m} \tau^n} - \frac{\binom{n+S_2m}{n} N_1}{\binom{n+S_2m}{n} \cdot n^{n+S_2m} \tau^n}
 \end{aligned}$$

213 **Properties**

214 The cases in which one N in C1-RDE is zero (or unknown) are called SLLs. The unknown cases
 215 cannot be calculated. However, if one term is zero, the SLLs are equivalent to C1-RDE (MLC);
 216 ALs are the acute stage ($N_2 > 0$ and $N_1 = 0$); and DLs denote the improved stage ($N_2 = 0$ and $0 <$
 217 N_1). In the unknown cases, the ALs indicate the present inflammation, whilst the DLs indicate
 218 the past inflammation. Even if the other terms present the kind of values, the size of the LC is
 219 larger if the injury is larger.

220 **SOC of the SLLs**

221 The SOC of the ALs (Figure 2) is the right first term of the RDE, and the other term is zero. The
 222 SOC of the DLs (Figure 3) is the right second term of the RDE. The tissue injury size is nearly
 223 equal to the size of the WSTL/WTL cluster (Section **MLC**). The SOC evaluates the SLLs
 224 (leukocyte cluster with the same τ , Figures 2 and 3), where N is the number, and τ is the fixed
 225 time.

226 An example of the ALs is (Figure 2, from AL0 in Figures 5A and S5–7):

$$227 \quad {}_{n+S_1m} \triangle_n \frac{N}{\tau} \equiv \frac{{}_{n-1} \triangle_n N_{2\tau}}{{}_{n-1} \triangle_n \tau} \equiv {}_{n+S_1m} \triangle_n \frac{N_{2, n+S_1m\tau_n}}{n+S_1m\tau_n} \equiv \frac{{}_{n+S_1m} \triangle_n \cdot N_{2\tau}}{{}_{n+S_1m} \triangle_n \cdot \tau}$$

228 An example of the DLs from AL1 is (Figure 3, from AL1 in Figures 5A and S5–7):

$$229 \quad {}_n \triangle_{n+S_2m} \frac{N}{\tau} \equiv \frac{{}_n \triangle_{n+1} N_{1\tau}}{{}_n \triangle_{n+1} \tau} \equiv {}_n \triangle_{n+S_2m} \frac{N_{1, n\tau_{n+S_2m}}}{n\tau_{n+S_2m}} \equiv \frac{{}_n \triangle_{n+S_2m} \cdot N_{1\tau}}{{}_n \triangle_{n+S_2m} \cdot \tau}$$

230 AL → DL (life → non-life):

$$231 \quad \triangle \rightarrow S_1, \quad (\triangle \rightarrow S_2)$$

$$232 \quad \text{AL} \rightarrow \text{DL}: \quad \frac{{}_{n+S_1m} \triangle_n \cdot N_{2\tau}}{{}_{n+S_1m} \triangle_n \cdot \tau} \rightarrow \frac{S_1 \cdot N_{2\tau}}{S_1 \cdot \tau} = \frac{S_1 \cdot N_{2t}}{{}_{n+S_1m} \triangle_n \cdot t}$$

233 In the case of the DL (Figure 3),

$$234 \quad S_1 \cdot \frac{N}{\tau} \equiv \frac{S_1 \cdot N_{1\tau}}{S_1 \cdot \tau} \equiv S_1 \cdot \frac{N_{1, n\tau_{n+S_2m}}}{n\tau_{n+S_2m}}$$

235 where a single value of $m = 1$ exists; τ is fixed time; t is real time; AL represents the active

236 leukocytes exhibiting a dynamic movement (Figure 2); and DL does not have a dynamic

237 movement (Figure 3). N is the number of leukocytes. τ_{n+m} is the phase time.

238 In the case of the AL ($\tau = 1$) (Figure 2):

$$239 \quad {}_{n+S_1 \cdot 1} \triangle_n N_{2\tau} \equiv {}_{n+S_1 \cdot 1} \triangle_n \frac{N_{2\tau}}{1} \equiv \frac{{}_{n+S_1 \cdot 1} \triangle_n N_{2\tau}}{{}_{n+S_1 \cdot 1} \triangle_n 1}$$

240 In the case of the DL (Figure 3):

241
$$S_1 \cdot N_{1\tau} \equiv S_1 \cdot \frac{N_{1\tau}}{1} \equiv \frac{S_1 \cdot N_{1\tau}}{S_1 \cdot 1}$$

242 The SLL has the same τ value ($m = 1$), and the size of the $S\tau C$ represents the size of the injury.

243 **MLC**

244 *SOC*

245 The SOC shows the size of the injury as an MLC:

246 The newer side term is $\frac{{}_{n-1}\Delta_n N_{2\tau}}{{}_{n-1}\Delta_n \tau}$, whilst the older side term is $\frac{{}_n\Delta_{n+1} N_{1\tau}}{{}_n\Delta_{n+1} \tau}$

247 In detail,

248 Newer side term:
$$\frac{{}_{n+S_1-1}\Delta_n \cdot N_2}{{}_{n+S_1-1}\Delta_n \cdot {}_{n+S_1-1}\tau_n},$$

249 Older side term:
$$\frac{{}_n\Delta_{n+S_2-1} N_1}{{}_n\Delta_{n+S_2-1} \cdot {}_n\tau_{n+S_2-1}}$$

250 In C1:
$$\frac{r dN_{\tau_n}}{r d\tau_n} = \frac{K}{Z} \frac{|N_{\tau}}{\tau} = \frac{{}_{n-m}\Delta_n N_{2\tau}}{{}_{n-m}\Delta_n \tau} - \frac{{}_n\Delta_{n+m} N_{1\tau}}{{}_n\Delta_{n+m} \tau} = \frac{{}_{n+S_1 m}\Delta_n N_{2\tau}}{{}_{n+S_1 m}\Delta_n \tau} - \frac{{}_n\Delta_{n+S_2 m} N_{1\tau}}{{}_n\Delta_{n+S_2 m} \tau}$$

$$251 \quad = + \frac{{}_{n+S_1m} \Delta_n \cdot N_{2\tau}}{{}_{n+S_1m} \Delta_n \cdot \tau} + \frac{{}_n \Delta_{n+S_2m} \cdot N_{1\tau}}{{}_n \Delta_{n+S_2m} \cdot \tau} \quad (C3)$$

$$252 \quad \tau_{n+S_1m} = \tau \cdot (n + S_1m), \quad \tau_{n+S_2m} = \tau \cdot (n + S_2m),$$

253 The numbers of leukocytes N_2 and N_1 and ${}_{n-m} \Delta_n \tau$ and ${}_n \Delta_{n+m} \tau$ as the phase time are
 254 extracted from the LC as $S\tau C$ in Figure 5A by a biological activity time chart by leukocytes
 255 (Figure S8) (example of the time is “ $\tau = 1$, $\Delta \tau = 1$ in LF, and $\Delta \tau = -1$ in RF”; Definition
 256 S3). When a newer side term ($m = 1$) represents a core leukocyte, the size of the injury is
 257 represented by this as the LC (Table S2). $S\tau C$ is the same as a CS that is equivalent to deform the
 258 dependent-variable-axis of the orthogonal-CS (Figure 6).

259 Fluctuation velocity (Kyoku) (γN)

260 The fluctuation in the velocity is described by C1-RDE:

$$261 \quad \frac{\frac{K}{Z} |N_\tau}{| \tau } = \frac{{}_{n-1} \Delta_n N}{{}_{n-1} \Delta_n \tau} - \frac{{}_n \Delta_{n+1} N}{{}_n \Delta_{n+1} \tau} = \frac{{}_{n+S_1m} \Delta_n \cdot N_{2\tau}}{{}_{n+S_1m} \Delta_n \cdot \tau} - \frac{{}_n \Delta_{n+S_2m} \cdot N_{1\tau}}{{}_n \Delta_{n+S_2m} \cdot \tau} = \gamma N$$

262 The inflammatory condition of each area of the τ zone is given as follows:

- 263 1) An older zone being the same size as a newer zone represents a chronic stage: $\{N_2 = N_1$ (each
 264 $N \neq 0\}$.
- 265 2) If a newer zone is smaller than an older zone, inflammation is in the improving stage: ($N_2 <$

266 N_1).

267 3) If a newer zone is larger than an older zone, the inflammation progresses to an acute stage (N_2

268 $> N_1$).

269 4) γN is visualized (SOC) (Definition S6.2).

270 γ in OOC (in C1, C2 and C3 RDEs)

$$271 \quad \gamma = \left(\frac{-\underset{n-m}{\Delta}_n N_\tau - \underset{n}{\Delta}_{n+m} N_\tau}{\underset{n-m}{\Delta}_n \tau - \underset{n}{\Delta}_{n+m} \tau} \right) \frac{1}{N} = \left(\frac{-\underset{n+S_1 m}{\Delta}_n \cdot N_{2\tau} - \underset{n}{\Delta}_{n+S_2 m} \cdot N_{1\tau}}{\underset{n+S_1 m}{\Delta}_n \cdot \tau - \underset{n}{\Delta}_{n+S_2 m} \cdot \tau} \right) \frac{1}{N}$$

272 The usual absolute value operator is as follows:

$$273 \quad \left| \underset{n}{\Delta}_n \right| = \underset{n}{\Delta}_n = +1, \quad \left| \underset{n}{\Delta}_n \right| = \underset{n}{\Delta}_n = -1$$

$$274 \quad |+1| = +1, \quad |-1| = +1$$

275 The relative absolute value operator (relative absolute operator):

$$276 \quad \left| \underset{n}{\Delta}_n \right| = +1, \quad \left| \underset{n}{\Delta}_n \right| = +1$$

277 The relative absolute value is as follows:

$$278 \quad N = \left(\left| -\underset{n-m}{\Delta}_n N_\tau \right| + \left| -\underset{n}{\Delta}_{n+m} N_\tau \right| \right) \cdot 1/2$$

$$279 \quad \gamma = \left(\frac{-\underset{n-m}{\Delta}_n N_\tau - \underset{n}{\Delta}_{n+m} N_\tau}{\left| -\underset{n-m}{\Delta}_n N_\tau \right| + \left| -\underset{n}{\Delta}_{n+m} N_\tau \right|} \right) \frac{2}{\tau}$$

280
$$N_{\tau_n} = N_0 \cdot \exp(\gamma_{\tau_n} \cdot \tau_n)$$

281 N_0 is the initial value; $\gamma = 0$ is the chronic stage (each $N \neq 0$); $\gamma < 0$ in C1 is the acute stage; $\gamma > 0$
 282 in C1 is the improving stage (RF); $\gamma < 0$ in C2 is the improving stage; and $\gamma > 0$ in C2 is the acute
 283 stage (RF and LF).

284 **γ of SLLs**

285 The SLLs cannot be used to obtain the solution if there is no other term. In contrast, $\gamma = 0$ is the
 286 chronic stage if there is a term (the term is zero). C1-RDE: $\gamma = S_1(+2)$ is the acute stage ($N_2 > 0$,
 287 $N_1 = 0$); $\gamma = S_1(-2)$ is the improving stage ($N_2 = 0$, $0 < N_1$; RF); C2-RDE: $\gamma = S_2(-2)$ is the
 288 improving stage ($N_2 > 0$, $N_1 = 0$); and $\gamma = S_2(+2)$ is the acute stage ($N_2 = 0$, $0 < N_1$; RF and LF).

289 **Antigen antibody reaction** (background is Text S7)

290 The fluctuation of γ according to an antigen–antibody reaction is presented as follows (C4,

291 Definition S6):

292
$$\frac{\frac{K}{n} \Big|_{1N_{\tau}}}{\frac{K}{n} \Big|_{\tau}} = \frac{r \Big|_{1N_{\tau_n}}}{r \Big|_{\tau_n}} = \frac{r d \Big|_{1N_{\tau_n}}}{r d \Big|_{\tau_n}} = \frac{\frac{\Delta}{\Delta} \Big|_{n \ 2N_{\tau}} \cdot \varepsilon_{21}}{\frac{\Delta}{\Delta} \Big|_{n \ \tau}} + \frac{\frac{\Delta}{\Delta} \Big|_{n \ 1N_{\tau}}}{\frac{\Delta}{\Delta} \Big|_{n \ \tau}}$$

293
$$\frac{\frac{K}{n} \Big|_{2N_{\tau}}}{\frac{K}{n} \Big|_{\tau}} = \frac{r \Big|_{2N_{\tau_n}}}{r \Big|_{\tau_n}} = \frac{r d \Big|_{2N_{\tau_n}}}{r d \Big|_{\tau_n}} = \frac{\frac{\Delta}{\Delta} \Big|_{n \ 2N_{\tau}}}{\frac{\Delta}{\Delta} \Big|_{n \ \tau}} + \frac{\frac{\Delta}{\Delta} \Big|_{n \ 1N_{\tau}} \cdot \varepsilon_{12}}{\frac{\Delta}{\Delta} \Big|_{n \ \tau}}$$

294 $1N$ depicts the leukocytes; $2N$ indicates the infective antigen (bacteria or microorganisms); ε is an

295 interference coefficient; ε_{12} is the phagocyte number coefficient pertaining to the leukocytes; and

296 ε_{21} is an invocation (cytokine) coefficient of the leukocytes to an antigen.

297

$${}_1\gamma_{\tau_n} = \frac{\varepsilon_{21} \cdot {}_{n-1}\Delta_n \cdot {}_2N_{\tau} + {}_n\Delta_{n+1} \cdot {}_1N_{\tau}}{\left| \varepsilon_{21} \cdot {}_{n-1}\Delta_n \cdot {}_2N_{\tau} \right| + \left| {}_n\Delta_{n+1} \cdot {}_1N_{\tau} \right|} \cdot \frac{2}{\tau}$$

298

$${}_2\gamma_{\tau_n} = \frac{{}_{n-1}\Delta_n \cdot {}_2N_{\tau} + \varepsilon_{12} \cdot {}_n\Delta_{n+1} \cdot {}_1N_{\tau}}{\left| {}_{n-1}\Delta_n \cdot {}_2N_{\tau} \right| + \left| \varepsilon_{12} \cdot {}_n\Delta_{n+1} \cdot {}_1N_{\tau} \right|} \cdot \frac{2}{\tau}$$

299 ${}_1N_0$ is the initial value of leukocyte, and ${}_2N_0$ is the initial value of bacteria:

300

$${}_1N_{\tau_n} = {}_1N_0 \cdot \exp({}_1\gamma_{\tau_n} \cdot \tau_n)$$

301

$${}_2N_{\tau_n} = {}_2N_0 \cdot \exp({}_2\gamma_{\tau_n} \cdot \tau_n)$$

302 The τ ratio (τ_r) is used if the reaction time of existence 1 (${}_1N$) and existence 2 (${}_2N$) is different:

303

$${}_1N_{\tau_n} = {}_1N_0 \cdot \exp({}_1\gamma_{\tau_n} \cdot \tau_n / \tau_r)$$

304 As a result, a stable solution is obtained (Figure 7). The conventional SDE was unstable by

305 above different-object interference (AO), and the solution described vibration and rotation,

306 where the new SDE successfully converges. Therefore, the future of inflammation becomes

307 clear.

308

309 **IMPLEMENTATION**

310 **StrLC**

311 The SOC simultaneously presents size and form. Time is calculated by the OOC; hence, the SOC
 312 is inaccurate.

313 **ALs:**
$$\left(\frac{\Delta_{n-m} \Delta_n \cdot 1}{\Delta_{n-m} \Delta_n \cdot \tau} \right) = \frac{\Delta_{n+S_1m} \Delta_n \cdot 1}{\Delta_{n+S_1m} \Delta_n \cdot \tau} = \frac{\Delta_{n+S_1m} \Delta_n \cdot N_2}{\Delta_{n+S_1m} \Delta_n \cdot t}$$

314 t : physical time

315 Size:

316
$$D \left(\Delta_{n-m} \Delta_n \right) \cong \Delta 15 \mu m, \quad \left| \Delta 1 \cdot \emptyset \right| \cong 15 \mu m$$

317 | is RAO, $\emptyset \cong 15 \mu m$ (Table S3)

318 The tissue injury size is $N_{2\tau} = 1$. The size is the same as WSTL/WTL (Figures 2, 4 and S4 B,

319 C, D, and H). The space information was constant, whilst the time information was variable.

320 Therefore, the form of the injury predicted from this StrLC form is the injury of a pipe-like form

321 of approximately 15 μm in diameter.

322 **OOC**

323 The transition from stage AL1s to AL2s (Figure S8) took 28 min (Table S4). ($m = 1, N = 1$)

324
$$v_m = \frac{\Delta \emptyset}{t} = \frac{\Delta 15}{\Delta (28/60)} = \frac{\Delta 32}{\Delta \cdot 1}$$

325
$$\left| \frac{\Delta_{32}}{\Delta_1} \right| = 32 \quad (\text{with RAO}), \quad \left(\frac{\Delta_{32}}{\Delta_1} = \Delta_{32} = -32 \text{ without RAO} \right)$$

326 Accordingly, $\phi = 15 \mu\text{m}$ (Table S3). The velocity is $\Delta_7 \mu\text{m/h}$. The tissue injury size is 15
 327 μm (constant). The transition from stage AL0s to AL1s took 4 h 24 min (264 min, Table S4) at
 328 $3.4 \mu\text{m/h}$.

329 **Conventional problem observed from StrLC SOC and OOC**

330 The dynamic information for this StrLC included time and cell injury information. The tissue
 331 injury information was constant. Using StrLC, we could understand the problem of observation
 332 via a one-cell unit, which enabled us to elucidate the problem of Lcnt and FCM.

333 **SLL**

334 *SOC*

335 τ is the phase time in Figure 2 ($\tau = 1$). The SOC can be located with SOC1, SOC2 and SOC3 in
 336 order of thinking. You will realise the size of inflammation and the future stage by the SOCs.

337 **SOC1: Injury form**

338 A figure (graph) of $\text{DN} \left(\frac{\Delta_{n-1} \Delta_n N_\tau}{\Delta_{n-1} \Delta_n \tau}, x, y \right)$ is in each envelope (white closed line) in Figure S4.

339 x and y denote the microscope images on a 720×480 -pixel orthogonal-CS. The other variables
 340 are the same as the SOC3.

341 **SOC2: Injury size**

$$342 \quad \left| \frac{\triangle_{n+S_1 \cdot 1} \triangle_n N_\tau}{\triangle_{n+S_1 \cdot 1} \triangle_n \tau} \right| = \left| \frac{\triangle_{n-1} \triangle_n \cdot N_\tau}{\triangle_{n-1} \triangle_n \cdot 1} \right| = [4, 8, \text{ and } 99] \text{ (Fig. 2 G, K, and O),}$$

343 $||$ is RAO

344 **SOC3: Graph of size and form**

$$345 \quad \triangle_{n+S_1 \cdot 1} \triangle_n \frac{N_\tau}{\tau} = \triangle_{n-1} \triangle_n N_\tau = \triangle_n \cdot (+4, +8 \text{ and } +99)$$

346 is the acute stage. The injury size is the SOC 2. The injury form is SOC1.

347 **OOC as a part of C1-RDE (MLC)**

348 If the other term is zero, $\gamma = -2 = S_{12}$ is the acute stage ($N_2 > 0, N_1 = 0$; Figure 2). Figure 3 shows

349 the improving stage ($\gamma = +2 = S_{22}; N_2 = 0, N_1 > 0$).

350 **MLC**

351 **SOC** (Applied data: Figures 5A and S5–S7, Table S2)

352 **SOC 1 Injury form:**

$$353 \quad \text{Figure (graph) of DN} \left(\frac{\triangle_{n-m} \triangle_n N_{2\tau}}{\triangle_{n-m} \triangle_n \tau}, x, y \right), \text{ and DN} \left(\frac{\triangle_n \triangle_{n+m} N_{1\tau}}{\triangle_n \triangle_{n+m} \tau}, x, y \right)$$

354 based on the insets (white closed line) in Figure S6.

355 The upper term is the number of leukocytes (size), whilst the lower term denotes a certain τ zone

356 of one leukocyte cluster.

357 **SOC 2:** Injury size (Table S2)

$$358 \quad \left| \frac{\triangle_{n-1} \triangle_n N_{2\tau}}{\triangle_{n-1} \triangle_n \tau} \right| = \frac{476}{1} = 476 \quad (\text{Figure S6 red dots as area 1})$$

$$359 \quad \left| \frac{\triangle_n \triangle_{n+1} N_{1\tau}}{\triangle_n \triangle_{n+1} \tau} \right| = \frac{286}{1} = 286 \quad (\text{Area 2 in Figure S6})$$

360 $\tau=1$, | | is RAO; the core is area 1 (red dots); and outside is area 2.

361 **SOC 3:** graph of size and form injury:

362 **Area 1 (AL core)**

$$363 \quad \frac{\triangle_{n+S_1-1} \triangle_n N_{2\tau}}{\triangle_{n+S_1-1} \triangle_n \tau} = \frac{\triangle_{n-1} \triangle_n N_{2\tau}}{\triangle_{n-1} \triangle_n \tau} = \frac{\triangle_{476}}{\triangle_1} = \triangle_{476}$$

364 **Area 2**

$$365 \quad \frac{\triangle_{286}}{\triangle_1} = \triangle_{286}$$

366 The figure (graph) is the result of the RDE of areas 1 and 2, and one may be able to count in a
 367 moment in this graph (as **SOC1-3**).

368 **SOC 4:** Fluctuation velocity and γN ; Kyoku

369 From Table S2 ($N_2 = 476$, $N_1 = 286$):

$$370 \quad \frac{\overset{\Delta}{\triangle}_{n-1} N_{2\tau} - \overset{\Delta}{\triangle}_n N_{1\tau}}{\overset{\Delta}{\triangle}_{n-1} \tau - \overset{\Delta}{\triangle}_n \tau} = \frac{\overset{\Delta}{\triangle}_{n-1} 476 - \overset{\Delta}{\triangle}_n 286}{\overset{\Delta}{\triangle}_{n-1} 1 - \overset{\Delta}{\triangle}_n 1} = \left| (S_1 \cdot 190) \right|_n = \left| (190) \right|_n$$

371 The fluctuation velocity value (γN) of Kyoku is $\{(S_1 190)\}$, representing the acute stage. γN is
 372 visualized (SOC).

373 **OOC**

374 Table S2 shows that γ was $\{(-0.5) = \{(S_1 0.5)\}$ in C1 (RF), representing the acute stage.

$$375 \quad N_{\tau_n} = N_0 \cdot \exp(\gamma_{\tau_n} \cdot \tau_n)$$

$$376 \quad 777 = 286 \cdot \exp(0.5 \cdot 2), \quad 785 = 476 \cdot \exp(0.5 \cdot 1), \quad 472 = 286 \cdot \exp(0.5 \cdot 1)$$

377 S_1 is the abbreviation. This equation is discovered as gsOOC in a part of SOC LC in Figures 5A
 378 and S7, and will be presented as a bar graph or a line graph. Naturally, γ of an antigen is
 379 required.

380 **Antigen–antibody reaction (prey and new predator) (C4-CS)**

381 *SOC (Figures S11 and S12)*

382 The display of the number of bacteria in a certain τ time and the number of leukocytes in the τ
 383 time were pseudo-SOC because ‘ ε ’ could not be used for the SOC. Moreover, the number of
 384 bacteria was not accurate in this case. Therefore, the SOC was also inaccurate. In the future, the
 385 display of SOC must be improved, and ‘ ε ’ must be used for the SOC.

386 *OOC (Figure 7)*

387 The solid lines depict the bacteria, whilst the dashed lines depict the leukocytes.

388 As an example, $\gamma_b = |S_1|0.50$ (Table S2, S1_Supporting Information); $\gamma_g = |S_2|0.25$ (Marsh
389 et al., 1994); $\varepsilon_{21} = 0.5$ (ε_{21} : arbitrary numbers were substituted; the appropriate number will be
390 determined in future studies); $\varepsilon_{12} = 250$ (Phagocytosis Assay Kit,
391 <https://www.funakoshi.co.jp/contens/3695>); $f_2(\tau)$ is the number of bacteria; and $f_1(\tau)$ is the
392 number of leukocytes. The relative τ ratio (τ_r) is 1.3 (1:1.3; τ_r : arbitrary numbers were
393 substituted; the appropriate number will be determined in future studies). Accordingly, $\tau = 10$ at
394 the time of interfere. The number of antigens was set to 0 when the antigen was set to 0.

395 The dissolution of the AO and the RO singularity using view-operator was successful
396 for the OOC.

397

398 **DISCUSSION**

399 As mentioned earlier, the RDE is put in the brain. When observing Figures 2 to 5 and Figures S4
400 to S7, one will recognise having become Dr. Perio (specialist periodontist), with the Perio eye
401 (periodontal-diagnostic doctor's eye) by the SOC and gsOOC. Accordingly, the SOC has a
402 real-time property. No 'model' exists, and no complicated property, like OOC, calculates the
403 solution. The SOC will educate A.I. and the young doctor. Furthermore, the OOC from the SOC
404 will extend it more precisely.

405 Conventional science only has the OOC; therefore, science has various problems. The
406 problems of cOOC are also mostly shown by the SOC, and will mostly be solved by the SOC. At
407 such time, the LC was found as the SOC in the periodontitis examination at the clinic. An
408 example is the inflammation, in which cell information from cOOC has problems. Therefore,
409 inflammation is described by the SOC and a new OOC from the SOC. Moreover, the LC as the
410 RDE, which realises the SOC, solves the problems of structural bioinformatics and enables the
411 measurement of local inflammation:

412 **1)** The SOC (LC) has the structure of bio-information, which can measure the space of the
413 inflammation in time. Therefore, it solves the problem of cell injury (cell information) and tissue
414 injury (tissue information).

415 **2)** The SOC LC exhibits no destruction of the structure of bio-information by conservative
416 sampling.

417 **3)** The SOC as LC by the RDE has the smoothness of differentiation.

418 **4)** The C4-RDE is a stable SDE.

419 **5)** Therefore, the observing eyes of the scientist and the doctor are considered to be the RDE,
420 which consist of primitive-operators, or the primitive-operators themselves.

421 In the future, the SOC will show us not only inflammation, but elementary particle, the life
422 and the new figure of the space–time continuum. Additional details have been provided below.

423 The diagnosis of the inflammation by the SOC is equivalent to the diagnosis of a new
424 OOC from the SOC. However, the SOC already had the result when the sample was obtained.
425 Accordingly, except for the manufacturing time, the calculation time of SOC is zero. If the
426 calculation time is zero, the computer has $P = NP$ property (Cook, 2000). Moreover, the
427 relationship between gsOOC(s) and SOC is $P = NP$ (Figure S7). A (conventional) computer does
428 not include the manufacturing time in the calculation time.

429 The LCs (StrLC, SLL and MLC) described above accurately present cell and tissue
430 injuries. Space information is represented by an empty space in a healthy tissue. The invasion is
431 greater if the empty space is larger (even if the extent of cell injury is the same).

432 The analytical methods used in modern pathology are systems, in which cells are
433 individually analysed. These approaches, including FCM, destroy tissue injury information.
434 Transferring these concepts to inflammation assessment requires the measurement of leukocyte
435 cluster information before the FCM because the FCM destroys the cluster of inflammatory cells.
436 Importantly, the Lcnt destroys a cluster similarly.

437 WTLs and WSTLs combine when in close proximity, and a larger leukocyte cluster
438 arises from a larger injury (be careful of the amount of supply of leukocytes). In contrast, a large
439 cluster does not derive from a small injury. Therefore, the size of the leukocyte cluster (in a time
440 zone) is proportional to the volume of the injury (in a time zone). This allows use of a staining

441 solution to enable the observation of the changes in the injury in a time section and permits the
442 representation of the injury as an $S\tau C$ LC.

443 The 'EOM', including the NSE, can be easily applied in practice. However, such
444 application of this equation is associated with several problems from AO or RO. These problems
445 can be solved using the primitive-operator.

446 The SLL is a subset of the MLC. In the future, studies will be needed to analyse the
447 inner time for the SLL (to MLC). The MLC can be used as a biomarker for C3-RDE (and
448 C4-RDE). These RDEs are the SOC.

449 The volume of the injury at a certain time is proportional to the volume of the LC of the
450 same τ cluster. Therefore, the LC can be used to calculate the velocity of inflammation and the
451 antigen–antibody reaction. The RDE can operate the future, the past and the present of the LC.

452 Conventional mathematics, including the CDE, expresses only the world of S_2 .
453 Therefore, a function can be used only in the first quadrant, and the problem changes to one
454 associated with singularity and non-smoothness. If a function differentiates in the
455 conventional-CS, in which S_1 does not exist, a quadrant change is unnatural and not smooth. Str
456 is eternal even if the function differentiates at any time. If the function does not use an Str
457 operator (View operator), it cannot obtain smoothness.

458 The CDE is presented as follows:

459
$$f'(x) = \lim_{h \rightarrow 0} \frac{f(x+h) - f(x)}{h}$$

460 An example: $f(x) = ax^2$ in the RStr (S_1) side (Zai has inner Kyoku. S_1 or S_2 has no inner
461 Kyoku.).

462
$$\lim_{h \rightarrow 0} \frac{f(\triangle x + \triangle h) - f(\triangle x)}{\triangle h} = \lim_{h \rightarrow 0} (+2a\triangle x + a\triangle h) = +2a\triangle x \quad (\text{pC2})$$

463
$$\lim_{h \rightarrow 0} \frac{f(S_1x + S_1h) - f(S_1x)}{S_1h} = \lim_{h \rightarrow 0} (+2aS_1x + aS_1h)$$

464 $= +2aS_1x$ *A breakdown of continuum is a premise.*

465
$$\lim_{h \rightarrow 0} \frac{f(S_1x + S_1h) - f(S_1x)}{S_1h} = \lim_{h \rightarrow 0} (+2aS_1x + aS_1h) = +2aS_1x \quad (\text{pC4})$$

466 The limiting value in the CDE belongs in pC4 (Imaginary operator and value), which is a scale.

467 Zai (value) (pC2) is described by an italic character. Kyoku (value) (pC1), pC3, pC5 and pC4 are

468 described by standard characters. The correspondence to pC2 (real) from pC4 (imaginary) gives

469 Zai. Therefore, StrLC is a transient form from CDE to RDE.

470 The numerator is bundled as follows:

471
$$f(\triangle x + \triangle h) - f(\triangle x) = a \triangle x \triangle x + a \triangle h \triangle x + a \triangle x \triangle h + a \triangle h \triangle h - a \triangle x \triangle x$$

472
$$= a \triangle x \triangle x + 2a \triangle h \triangle x + a \triangle h \triangle h - a \triangle x \triangle x = +2a \triangle h x + a \triangle h^2$$

473 The denominator is bundled as follows:

474
$$\frac{+2a \triangle h x + a \triangle h^2}{\triangle h} = +2a \triangle x + a \triangle h$$

475 The relationship between the CS (StrZai) and the function is exact.

476 Str (S₂) side:

$$477 \quad \lim_{h \rightarrow 0} \frac{f(\Delta x + \Delta h) - f(\Delta x)}{\Delta h} = \lim_{h \rightarrow 0} (+2a\Delta x + a\Delta h) = +2a\Delta x$$

478 Exponent:

$$479 \quad e^{\Delta t} = \frac{d^x}{dt^x} e^{\Delta t} \quad x \text{ is integer}$$

$$480 \quad e^{\Delta t} = \frac{d^x}{dt^x} e^{\Delta t} = \frac{d^x}{dt^x} e^{+t} \quad x \text{ is integer}$$

$$481 \quad e^{-t} = \frac{d^x}{dt^x} e^{-t} \quad \text{If the number of } x \text{ is even}$$

482 The CDE cannot determine Kyoku; therefore, the singularity and the integration constant are
483 generated, allowing the convergence-differentiation using only one side of the CS.

484 If a conventional CS is established on an imaginary scale {imaginary-coordinate-system
485 [ICS] in pC4 (Definition S1.5)}, the function involves a factor that represents a view (particularly
486 Gv₁), with the tool used to solve it as the Str operator. The view will change if a function mixing
487 ‘-’ as the view (value) differentiates conventionally. This is unnatural and considered as the
488 cause of the smoothness problem associated with differentiation. We must not mix absolute
489 minus and relative minus without distinguishing them (i.e. relative operations _RStrZai and
490 _LStrZai). The RCS for natural science should be formed from StrZai (Figure 6), with this view
491 representing an observation. Therefore, the CS is the Zai (existence) itself and the observation.

492 (IDP-EOM is improved by the C3-CS. A different-object interference is improved by the C4-CS.

493 The NSE is improved by the C3-CS and/or C4-CS.)

494 The global view in a conventional-CS has to be distinguished from the function by the

495 Str operator (particularly $G_{V_1} = -$). The view is borrowed from the CS; hence, it must not be

496 changed by conventional convergence-differentiation and a conventional absolute-value-operator.

497 The conventional differential equation expresses only one side (${}_L$ Str area), and the smoothness of

498 a differential equation requires an Str operator similar to an EOM. The NSE is not equipped with

499 Str operators and not smooth under all circumstances. The perfect answer to the Clay Millennium

500 Problem (Fefferman et al., 2000) using the NSE is presented as follows:

501
$$\prod \triangle = \triangle$$

502 The limitations of the SOC, RDE, primitive-operators and $S\tau C$ (LC) are currently

503 unknown. Hence, research in this field should be continued to determine the limitations.

504

505 **ACKNOWLEDGEMENTS**

506 I would like to thank the staff at Nonomura Dental Clinic for their clinical assistance; Dr.

507 Sachiko Nisida and Dr. Hiroko Kamide for their assistance with language editing; Miss Haruko

508 Kobayashi, Miss Manami Niwa, Miss Miki Matsushita, and Mr. Keita Taki for reference

509 searches; and Mrs. Tomomi Okuda and Miss Saori Nishida for their assistance with the

510 photographs and figures.

511

512 **Microscopes**

513 The cover glass, slide glass, phase-contrast microscope and fluorescence microscope used herein

514 were general models ((Limited company, MicroDent, Japan).

515

516 **Conflicts of interest**

517 The author declares no conflicts of interest, except for the patents.

518

519 **Funding**

520 No external funding was used for this study.

521

522

523 **REFERENCES**

524 Britton, N.F. (2010) Essential Mathematical Biology. Springer-Verlag: London, UK, pp. 55–59.

525 Cook, S. (2000) The P versus NP problem. Available at:

526 <http://www.claymath.org/sites/default/files/pvsnp.pdf> (access October 25, 2018).

527 Cossarizza, A., et al. (2017) Guidelines for the use of flow cytometry and cell sorting in

- 528 immunological studies. *Eur J Immunol*, 47, 1584–1797.
- 529 Dacie, J. V. (1975) *Basic Haematological Techniques*, 4th edition, Leucocyte Counts, pp. 46–67.
- 530 Fefferman, C.L. (2000) Existence and smoothness of the Navier–Stokes equation. Available at:
- 531 <http://www.claymath.org/sites/default/files/navierstokes.pdf> (accessed October 25, 2018).
- 532 Flow cytometry technical information, Beckman Coulter Inc. Available at:
- 533 <https://www.bc-cytoh.com/cytometry.html> (accessed October 25, 2018).
- 534 George, E.C. (1968) *Diagnostic Laboratory Hematology*, 4th edition, Leukocyte Count, pp. 43–
- 535 48.
- 536 Hawkins, A., Cornell, H.V. (1999) *Theoretical Approaches to Biological Control*. Cambridge
- 537 University Press: Cambridge, UK, pp. 5–14.
- 538 How to count the number of cells by a blood-cell-counting board:
- 539 <https://m-hub.jp/biology/1277/how-to-count-the-number-of-viable-cells-using-a-hemocytometer>
- 540 <https://www.abcam.co.jp/protocols/counting-cells-using-a-haemocytometer-2>
- 541 <https://www.funakoshi.co.jp/contents/3075>
- 542 Krainov, V.P. (2002). *Selected Mathematical Methods in Theoretical Physics*. Taylor & Francis:
- 543 London and New York, pp. 165–176.
- 544 Lindhe, J. (2015) *Clinical Periodontology and Implant Dentistry*, Chapter 5, 6th edition.
- 545 Graham, M.D., et al. (2003) The Coulter Principle: Foundation of an Industry. *JALA*, 8:72-81,

546 <https://doi.org/10.1016/S1535-5535-03-0023-6>

547 Marsh, P.D., et al. (1994) The effect of growth rate and haernin on the virulence and proteolytic
548 activity of *Porphyromonas gingivalis* W50. *Microbiology*, 140, 861–865.

549 Ozmeric, N. (2004) Advances in periodontal disease markers. *Clin Chim Acta*, 343(1–2), 1–16.

550 Phagocytosis assay kit. Available at: <https://www.funakoshi.co.jp/contents/3695> (accessed October
551 25, 2018).

552 Preshaw, P.M. (2015) Detection and diagnosis of periodontal conditions amenable to prevention.
553 *BMC Oral Health*, 15, S5.

554 Rubin, R. (2007) Rubin’s Pathology, 5th edition, Lippincott Williams & Wilkins, a Wolters
555 Kluwer, Chapter 1, pp. 1–35.

556 Rubin, R. (2007) Rubin’s Pathology, 5th edition, Lippincott Williams & Wilkins, a Wolters
557 Kluwer, Chapter 2, pp. 37–70.

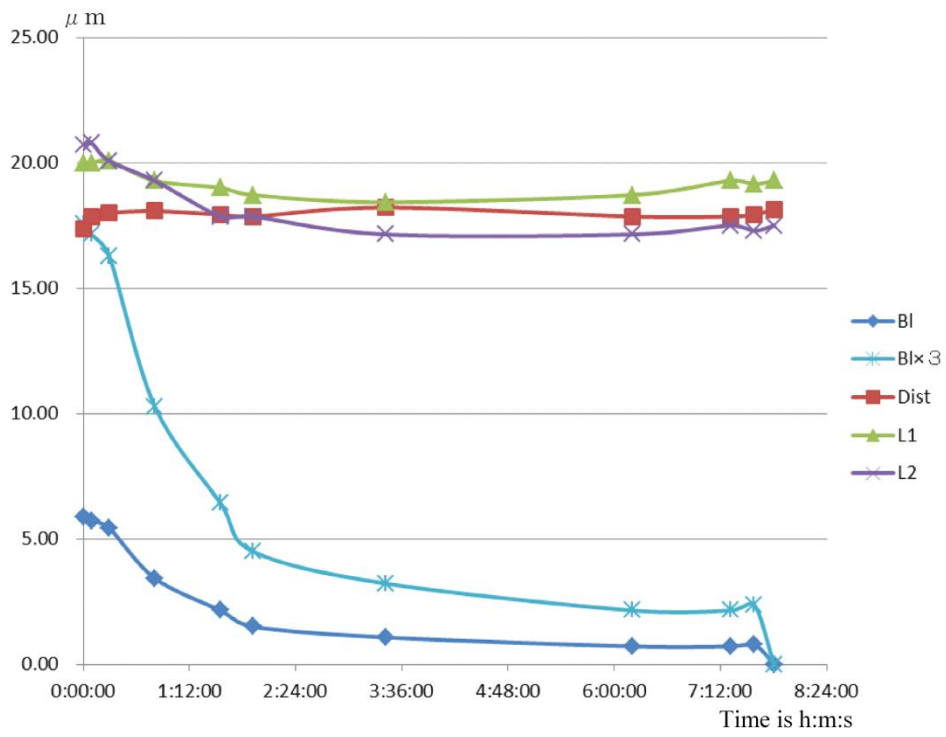
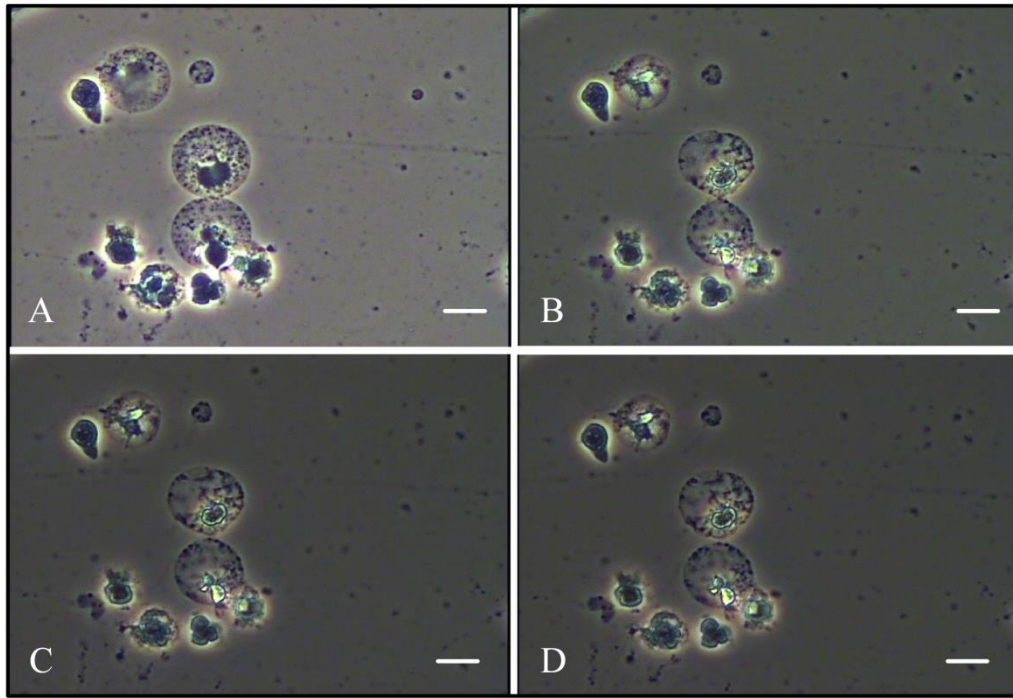
558 Saito, M., et al. (2002) Crevicular fluid PGE₂ used to evaluate the effect of initial preparation in
559 adult periodontitis. *Nihon Shishubyo Gakkai Kaishi*, 44, 131–147.

560 Saw, E.-W., et al. (2016) Experimental characterization of extreme events of inertial dissipation
561 in a turbulent swirling flow. *Nat Commun*, 7, 12466.

562 Talk CBC Vol. 1, Beckman Coulter Inc. Available at:
563 <https://www.beckmancoulter.co.jp/product/product02/cbc/vol01.html> (accessed October 25, 2018).

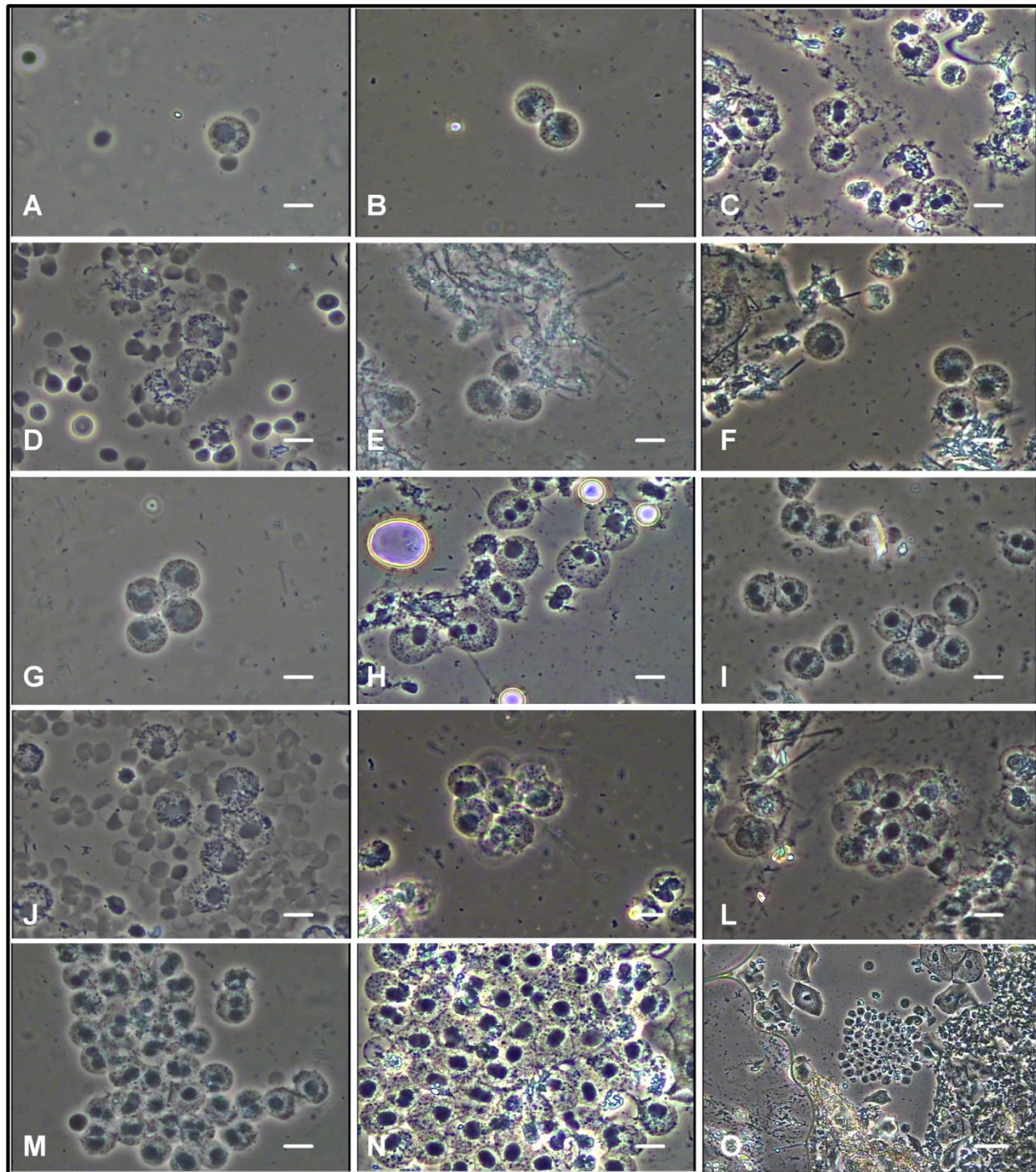
- 564 Teramoto, E., et al. (2009) Suuri Seitaiaku. Asakura Shoten: Tokyo, pp. 76–116.
- 565 The Japan Society of Ningen dock, WBC. Available at:
- 566 <https://www.ningen-dock.jp/public/inspection/blood> (accessed October 25, 2018).
- 567 Thornley, J.H.M., France, J. (2007). *Mathematical Models in Agriculture*, 2nd edition. CABI:
- 568 Wallingford, UK, pp. 227–228.
- 569

570 **Figure and Figure Legends**



571

572 **Figure 1. Leukocyte–dissociation curves.** (A) Time 0:00:00 is the start of the experiment. The
573 contact line (Figure S2) represents a primary bond. (B) Time 6:12:10 is the point after initial
574 dissociation. Coupling occurs via a secondary bond between two leukocytes. (C) Time 7:48:23 is
575 the point of secondary dissociation and bond breakage. (D) Time 8:01:37 is the point after
576 secondary dissociation. (A–D) Scale: 10 μm . (E) The bond length (Bl) describes the length of the
577 contact line formed by the primary and secondary bonds. Leukocyte 1 (L1) represents the upper
578 leukocyte diameter, whilst L2 represents the lower leukocyte diameter. The distance between L1
579 and L2 is denoted by ‘Dist’.



580

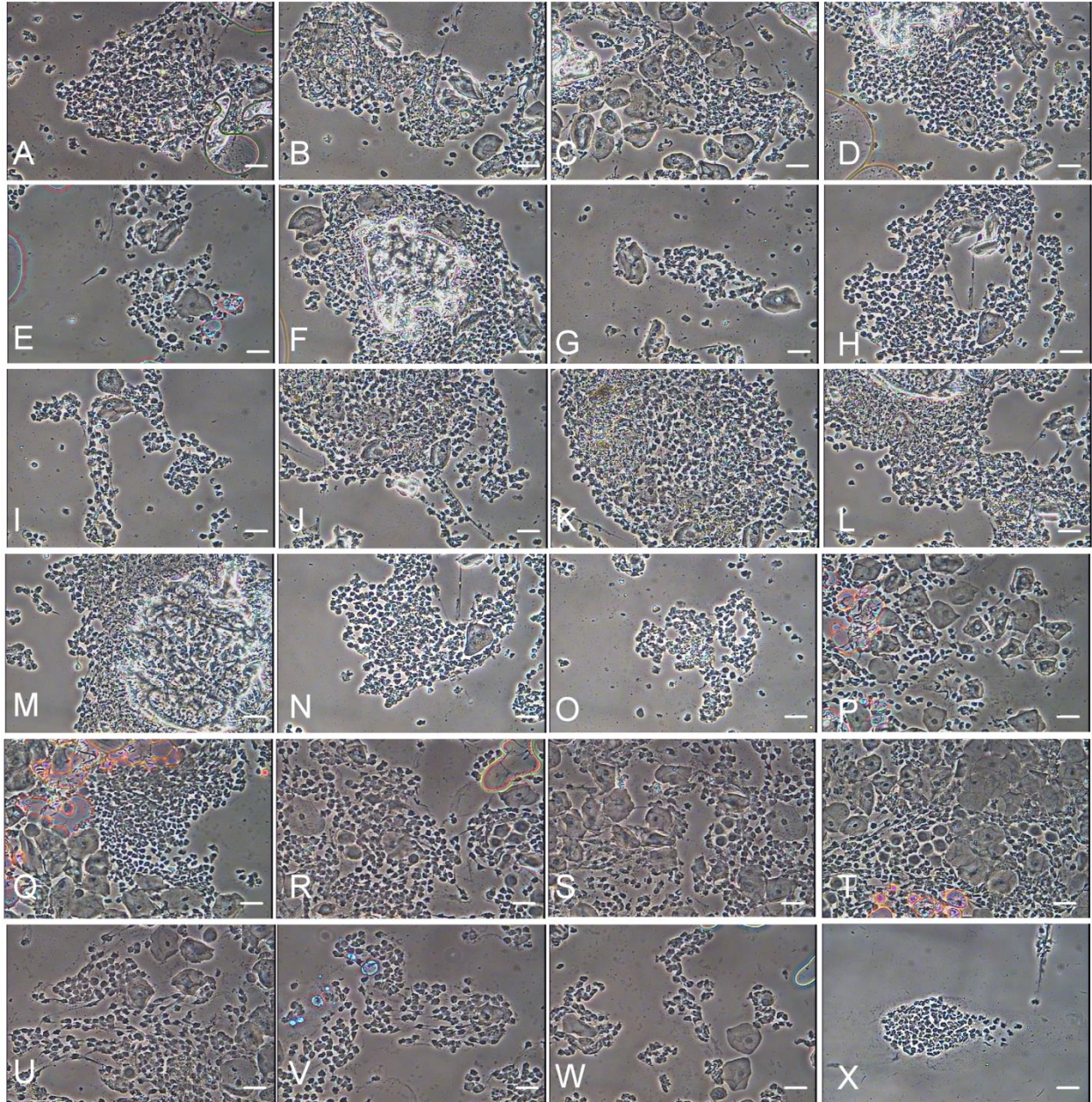
581 **Figure 2. AL clusters identified according to the dynamic movement of the organelles**

582 **following WTL. (A) Single and (B–O) multiple leukocyte clusters (A–N) Scale: 10 μ m and (O)**

583 40 μ m.

584 Before applying the RDE, 'Model' is seen as the CDE with many singularities. It is perceived as

585 SOC after RDE application.

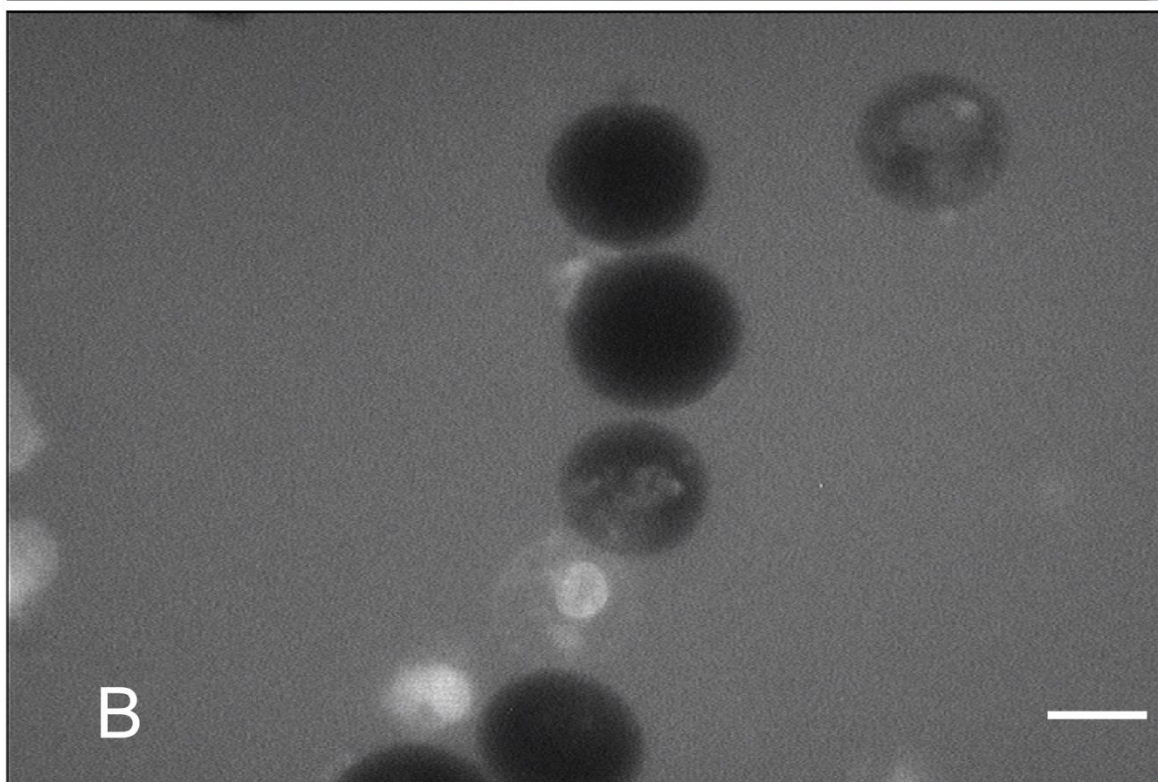
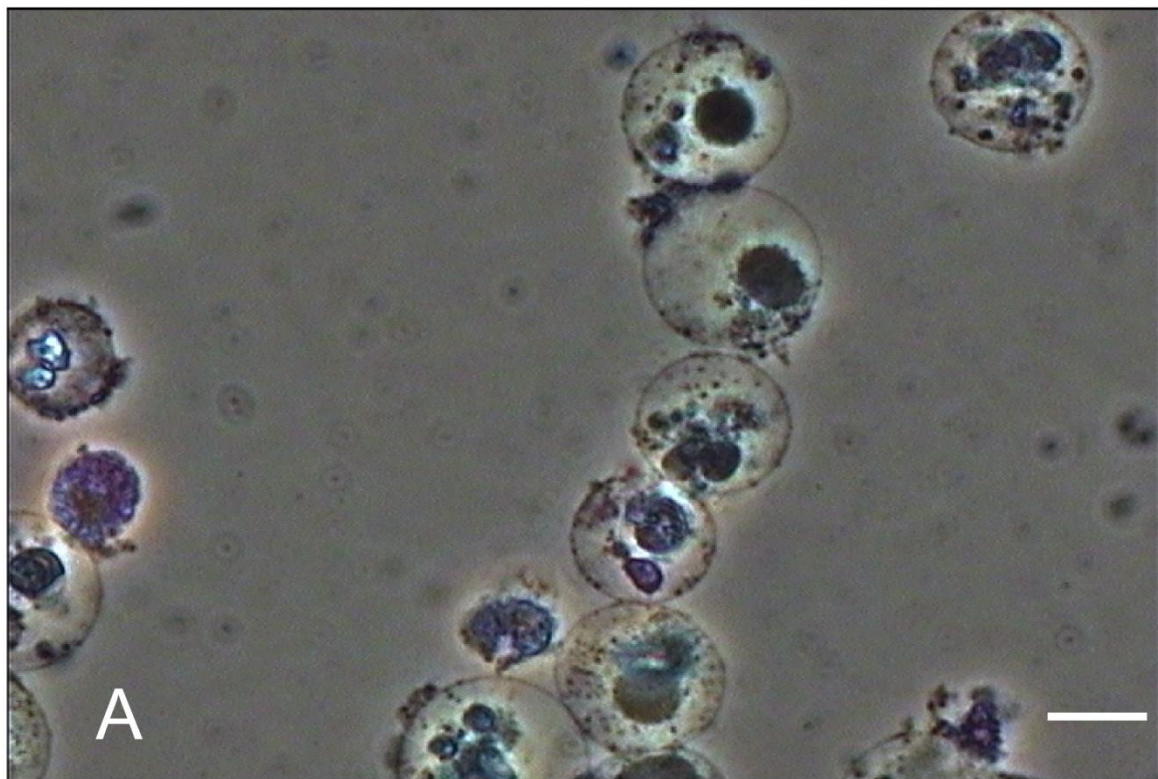


586

587 **Figure 3. DL clusters.** Destructive leukocytes (DL) clusters. Scale: 40 μ m.

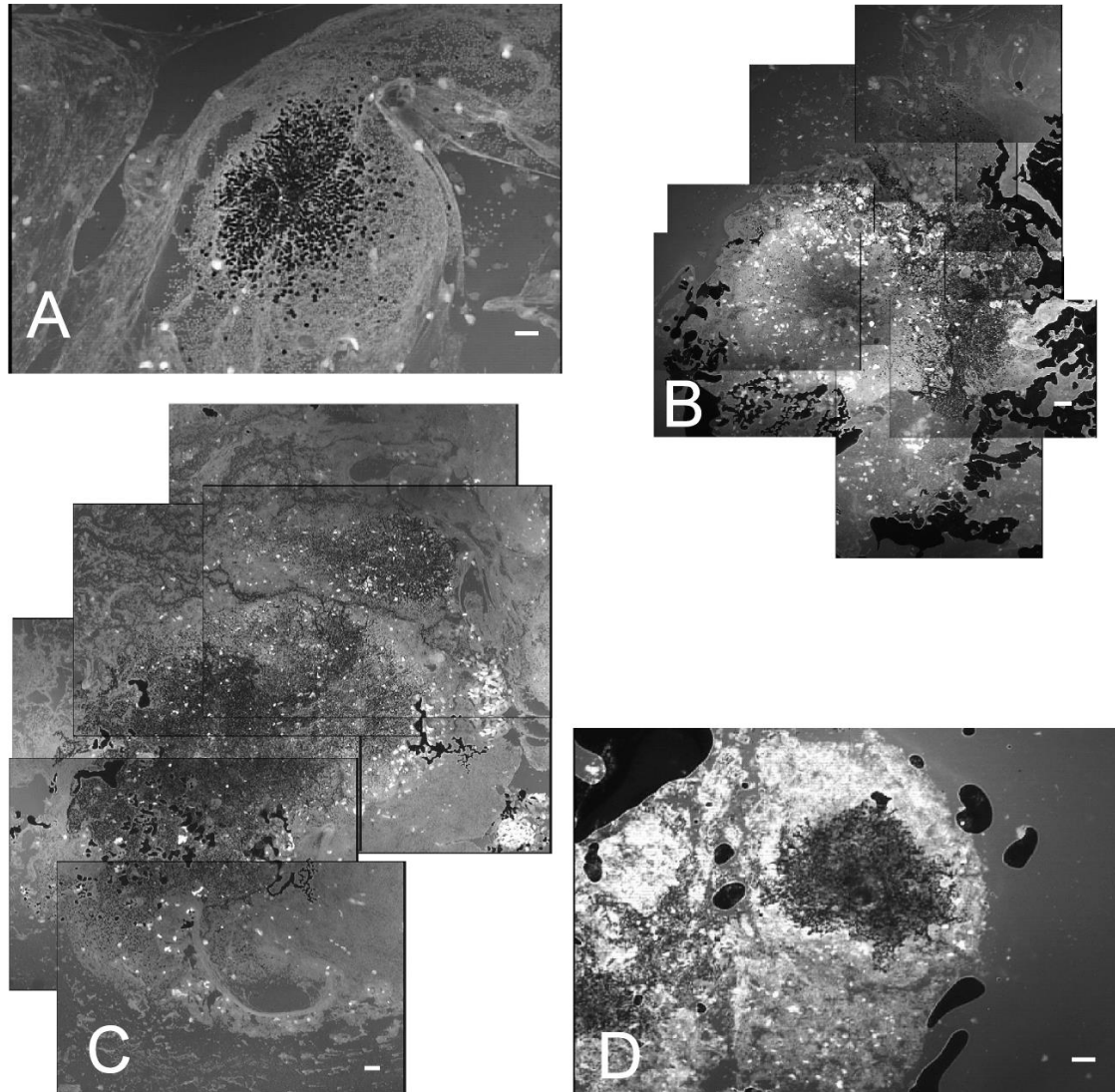
588 DL cannot be analysed by CDE. The analysis is possible for SOC. However, DL gradually loses

589 continuity. SOC also collapses according to it. However, DL is useful to diagnostics.



590

591 **Figure 4. StrLC by WSTL.** Results of the WSTL as measured by fluorescence. **(A)** Results of
592 the WSTL according to a phase-contrast observation. Older cells are white, whilst newer
593 leukocytes are black. Scale: 10 μm . **(B)** Results of the WSTL as measured by a fluorescence
594 mode observation. Older leukocytes are white, whilst newer leukocytes are black. Scale: 10 μm .
595 StrLC is a string function with a CS as an independent axis. AO- or RO-type singularity is
596 observed according to this function. StrLC shows us various problems, such as EOM and CET.
597 The calculation of AO or RO is possible using primitive-operator.



598

599 **Figure 5. MLCs as SrC by WSTL.** An AO-type singularity is observed at the centre of the

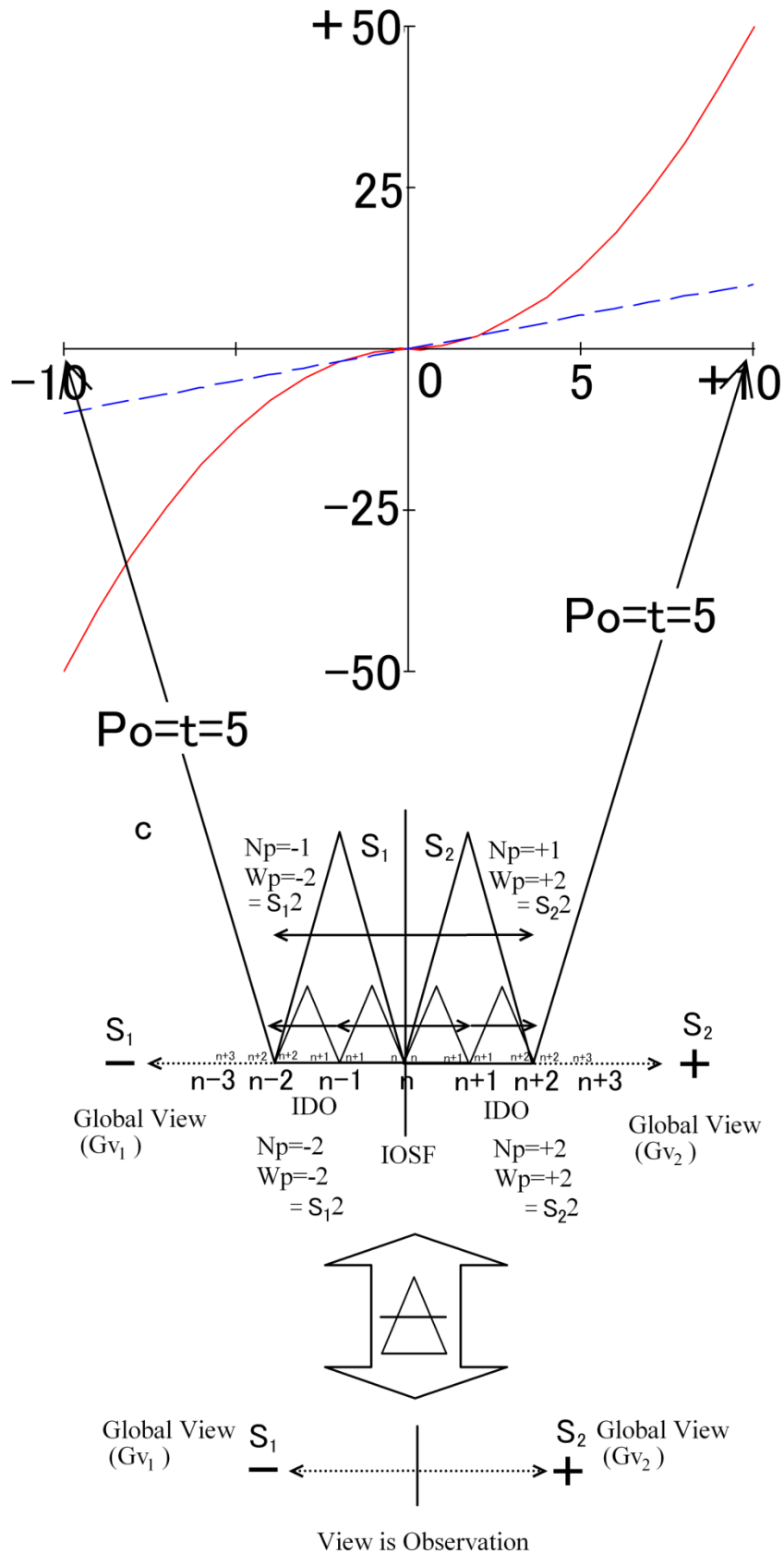
600 MLC. (A) Enclosure at the outermost periphery of a fibrous connective tissue indicating a

601 complete view of one tissue injury. Scale (A, C and D): 100 μm and (B) 200 μm . Before

602 applying RDE, 'Model' is perceived as the CDE with many singularities. After applying the RDE,

603 it is perceived as SOC. It has solution as OOC. MLC shows the complete SOC RDE. MLC can

604 observe gsOOC simultaneously.



606 **Figure 6. Real coordinate system.** Condition 3, coordinate system according to StrZai on the
 607 G-axis (horizontal axis). The orthogonal axis is the K-axis. Single StrZai ($N_p = S_1 \cdot 1 = -1$, $W_p =$
 608 $S_1 \cdot 2 = -2$) ($N_p = S_2 \cdot 1 = +1$, $W_p = S_2 \cdot 2 = +2$) and StrZai continuum ($N_p = S_1 \cdot 2 = -2$, $W_p =$
 609 $S_1 \cdot 2 = -2$) ($N_p = S_2 \cdot 2 = +2$, $W_p = S_2 \cdot 2 = +2$). P_o is time ($t = 5$).

610 red line: $\frac{1}{2}a(t\Delta)^2 \{_{R}Str\ side(S_1\ side)\}$, $\frac{1}{2}a(t\Delta)^2 \{_{L}Str\ side(S_2\ side)\}$ (C3),

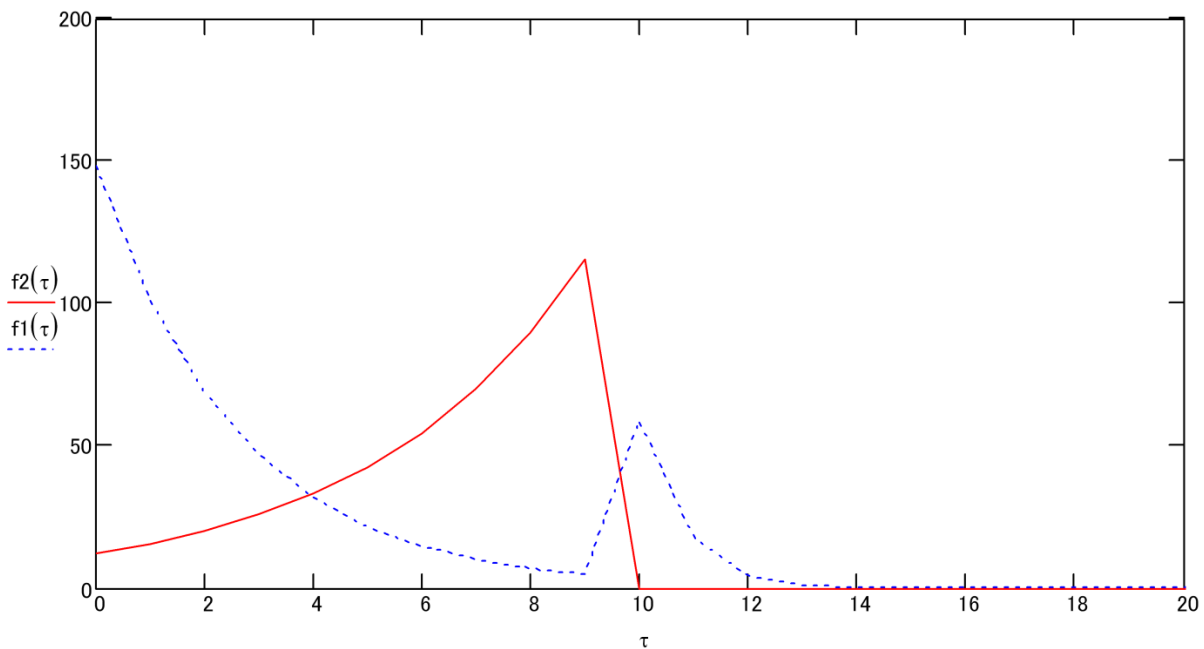
611 blue line: $v_0(t\Delta)^1 \{_{R}Str\ side(S_1\ side)\}$, $v_0(t\Delta)^1 \{_{L}Str\ side(S_2\ side)\}$ (C3),

612 $y_0(t\Delta)^0 + y_0(t\Delta)^0 = 0$, $y_0\Delta + y_0\Delta = 0 = |y_0\ at\ origin$ (C3)

613 $\frac{1}{2}a(t\Delta)^2 + \frac{1}{2}a(t\Delta)^2 = 0$, $v_0(t\Delta)^1 + v_0(t\Delta)^1 = 0$ (C3)

614 $t \geq 0$

615 The C3 coordinate system solves the problems of singularity, integration constant and initial
 616 value. The red (and blue) line denotes the ‘right line’.



617

618 **Figure 7. Antigen–antibody reaction according to Lotka–Volterra equations.** The solid line
619 represents bacteria, whilst the dashed line represents leukocytes.